References and Notes

1. L. E. Rosenberg in *The Metabolic Basis of Inherited Disease*, J. B. Stanbury *et al.*, Eds. (McGraw-Hill, New York, 1983), p. 474.
2. P. Youngdahl-Turner and L. E. Rosenberg, *J. Clin. Invest.* **61**, 133 (1978).
3. C. Bradbeer, in *Vitamin B_{12}*, B. Zagalak and W. Friedrich, Eds. (de Gruyter, New York, 1979), p. 711.
4. D. S. Rosenblatt, B. A. Cooper, A. Pottier, H. Lue-Shing, N. Matiaszuk, K. Grauer, *J. Clin. Invest.* **74**, 2149 (1984).
5. W. A. Gahl *et al.*, *Science* **217**, 1263 (1982).
6. W. A. Gahl *et al.*, *J. Biol. Chem.* **257**, 9570 (1982).
7. A. Dubin, A. Koj, J. Chudzik, *Biochem. J.* **153**, 389 (1976).
8. W. B. Chodirker, G. N. Bock, J. H. Vaughan, *J. Lab. Clin. Med.* **71**, 9 (1968).
9. This is publication 85007 from the McGill University Montreal Children's Hospital Research Institute.

* To whom requests for reprints should be sent at 2300 Tupper Street, A709 Montreal, Quebec H3H 1P3, Canada.

26 December 1984; accepted 22 February 1985

Correlated Measurements of DNA, RNA, and Protein in Individual Cells by Flow Cytometry

Abstract. *A cytochemical method was developed to differentially stain cellular DNA, RNA, and proteins with fluorochromes Hoechst 33342, pyronin Y, and fluorescein isothiocyanate, respectively. The fluorescence intensities, reflecting the DNA, RNA, and protein content of individual cells, were measured in a flow cytometer after sequential excitation by three lasers tuned to different excitation wavelengths. The method offers rapid analysis of changes in the cellular content of RNA and protein as well as in the RNA-protein, RNA-DNA, and protein-DNA ratios in relation to cell cycle position for large cell populations. An analysis of cycling cell populations (exponentially growing CHO cultures) and noncycling CHO cells arrested in the G_1 phase by growth in isoleucine-free medium demonstrated the potential of the technique.*

Flow cytometric analysis of DNA content in single cells provides a rapid and accurate method for determining the cell cycle frequency distribution of a given population (*1*). Determinations based on DNA content alone, however, cannot discriminate among the many metabolic states related to a cell's capacity to progress through the cell cycle. Distinctions between quiescent and cycling cells or among cells in various stages of differentiation, and the relation between cell growth and DNA division, can be better assessed by multiparametric analysis of DNA and RNA (*2*) or DNA and protein (*3*). For instance, in certain cell systems quiescent (G_0, G_1Q) or differentiating (G_1D) cells can be distinguished from cycling G_1 cells on the basis of RNA content (*4*). In other systems some cells may be characterized by an S-phase DNA content but may not traverse the S phase or traverse it very slowly; such cells (S_Q) can also be recognized by multiparametric analysis (*4*). A critical RNA content and, perhaps, also a protein content for cells in G_1 discriminates between two functionally distinct compartments of G_1, G_1A and G_1B, believed to have different roles in the cell cycle (*5*). To our knowledge, a method has not been found to measure simultaneously DNA, RNA, and protein in the same cells. Such measurements, especially when combined with an assessment of the ratio of RNA to DNA or RNA to protein per cell, can provide additional information on cell metabolism as related to cell cycle, quiescence, differentiation, transformation, or sensitivity to drug treatment, and may offer a new method for recognizing and classifying tumor cells.

We report here a flow cytometric method for the direct determination and correlation of DNA, RNA, and protein content in individual cells (*6*). The cytochemical reaction incorporates modified procedures for staining DNA with Hoechst 33342 (*7*), RNA with pyronin Y (PY) (*8*), and protein with fluorescein isothiocyanate (FITC) (*3*). Stained cells are analyzed with a three-laser excitation flow system (*9*).

One of the main difficulties in multicolor fluorescence analysis arises from the overlap in the fluorescence excitation and emission spectra of the individual dyes. With spatially separated laser beams, each set at a wavelength near the optimum for excitation of a given dye and appropriate filter arrangements, we have achieved good color separation. Figure 1 illustrates the analytical scheme used for analyzing three color–stained cells. The flow system is equipped with three lasers tuned to specified wavelengths and focused at points 250 μm apart on the cell stream, allowing preferential excitation and emission analysis of each dye over a preselected wavelength region and ensuring the fluorescence color resolution necessary for high sensitivity and accuracy. The three fluorescence signals and ratio signals, obtained with analog divider circuits (*10*), from each stained cell are collected and stored in correlated list mode in a Digital Equipment Corp. PDP11/23 computer (*11*) for subsequent analysis of DNA, RNA, and

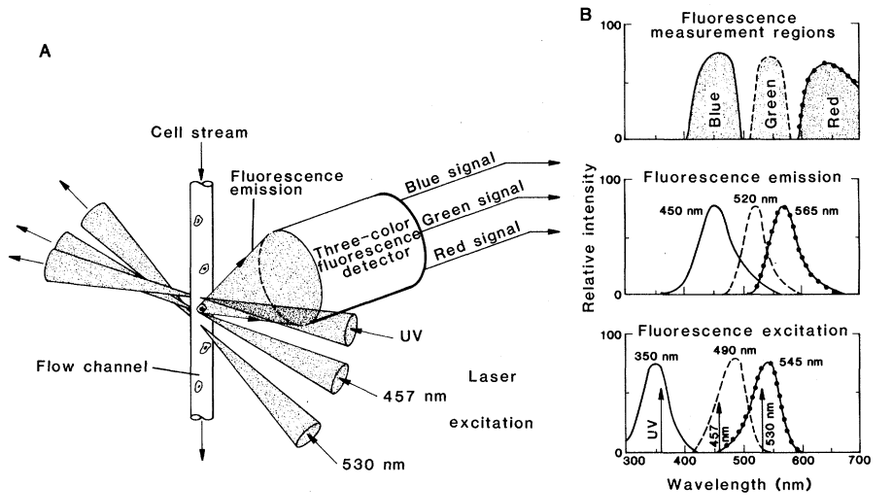

Fig. 1. (A) Three-laser excitation and fluorescence emission measurement scheme for analysis of DNA, RNA, and protein in three color–stained cells. The laser beams, tuned to the designated wavelengths, are spaced 250 μm apart. Excitation and emission analysis are thus performed preferentially for each dye at a different point on the cell stream. Measurements are correlated on a cell-to-cell basis. The three-color fluorescence detector consists of colored glass and dichroic color separating filters for measuring blue (400 to 500 nm), green (515 to 575 nm), and red (>580 nm) fluorescence emission from cells. Fluorescence signals, including ratio signals (*10*), are directed to signal-processing electronics for storage (correlated list mode) in a PDP11/23 computer (*11*) and subsequently are displayed as single-parameter frequency distribution histograms and two-parameter contour diagrams. (B) Fluorescence excitation and emission spectra and wavelength measurement regions for Hoechst 33342 (——), FITC (– – –), and PY (●). Arrows in the fluorescence excitation regions are laser beam wavelengths preselected for sequential excitation of each dye in stained cells.

protein content as well as ratios of RNA to DNA and RNA to protein on a cell-to-cell basis.

To test the reliability of the system for quantitative determinations of cellular DNA, RNA, and protein, we analyzed CHO cells stained with only one of each of the dyes or with all three dyes in combination. In all cases cells were excited by all three laser beams and fluorescence analysis was performed in the blue, green, and red channels to determine the degree of nonspecific fluorescence in each channel. The fluorescence of each dye was detected in the appropriate analysis channel; only in the case of cells stained only with PY was a minimal amount of fluorescence detected in the green (FITC) channel. This indicates that PY is excited to a very small extent also at 457 nm. Green fluorescence in three color–stained cells was slightly less intense than that observed when cells were stained with FITC alone, perhaps because of energy transfer from FITC molecules to PY. This was also reflected by a small increase in PY fluorescence. Enzyme studies have shown that approximately 90 percent of the PY fluorescence of CHO cells is sensitive to ribonuclease A, indicating a degree of stain specificity comparable to that of another RNA fluorochrome, acridine orange (*4, 5*). RNA content as measured in whole cells is mostly a reflection of ribosome concentration, since approximately 80 percent of the RNA in the average cell is ribosomal (*4*).

The technique was used to characterize exponentially growing as well as noncycling CHO cells in cultures deprived of isoleucine (*12, 13*). Isoleucine deprivation is a generally accepted method of achieving cell synchronization in G_1 (*13*), but the metabolic state of individual cells thus arrested has not yet been determined. The results, presented in Table 1 and Fig. 2, are for samples stained and analyzed on the same day. Experiments were repeated at least three times with similar results.

The patterns of cell distribution with respect to RNA and protein content were strikingly similar both in exponentially growing (Fig. 2A) and noncycling (Fig. 2B) populations. The populations, however, were more heterogeneous on the basis of protein than RNA content. This is evident from the width of the G_1, S, or G_2 + M clusters (Fig. 2) and from the standard deviations for these subpopulations (Table 1). The range in variability of the values in Table 1 is similar to that reported previously for the ratio of DNA to RNA (*8*) or DNA to protein (*14*).

The characteristic feature of the G_1 population was the presence of a threshold RNA or protein content (arrows in panels a and b of Fig. 2A). It is evident that cells with a subthreshold content of these macromolecules do not immediately enter the S phase. As described before (*5*), this threshold discriminates between G_1A and G_1B. The G_1A compartment represents the growth or "equalization" (competence) phase of the cycle, whereas during G_1B cells both grow and progress through the division cycle (*5*). In the exponentially growing population about half of G_1 cells were in G_1A (that is, were characterized by the subthreshold RNA or protein content) (panels a and b in Fig. 2A). There was a remarkably constant relation between the RNA and protein contents of individual cells in the cycling population (panel c in Fig. 2A). However, the threshold RNA or protein content in G_1, so evident in exponentially growing populations, is not an absolute requirement for entrance to the S phase (*15*).

Analysis of the RNA-DNA ratio (panel e in Fig. 2A) in relation to cell cycle position as represented by DNA content reveals a characteristic pattern of changing rates of DNA replication versus transcription. Thus during G_1, when DNA content was constant, cells accumulated increasing quantities of RNA, which is reflected by the high heterogeneity of the RNA-DNA ratio and by the fact that the late G_1 cells had a maximum RNA-DNA ratio before entering the S phase. The RNA-DNA threshold (arrow in panel e of Fig. 2A) indicates the previously discussed RNA threshold that cells must attain before they enter the S phase. During progression through that phase, the rate of DNA replication exceeded that of RNA accumulation, giving rise to a nonvertical, negative slope in the RNA-DNA ratio for the S phase cell cluster. Cells in G_2 + M had, on average, an RNA-DNA ratio similar to that of most G_1 cells.

The ratio of RNA to protein is a novel parameter for individual cells. Correlated measurements of DNA, RNA, and protein make it possible not only to

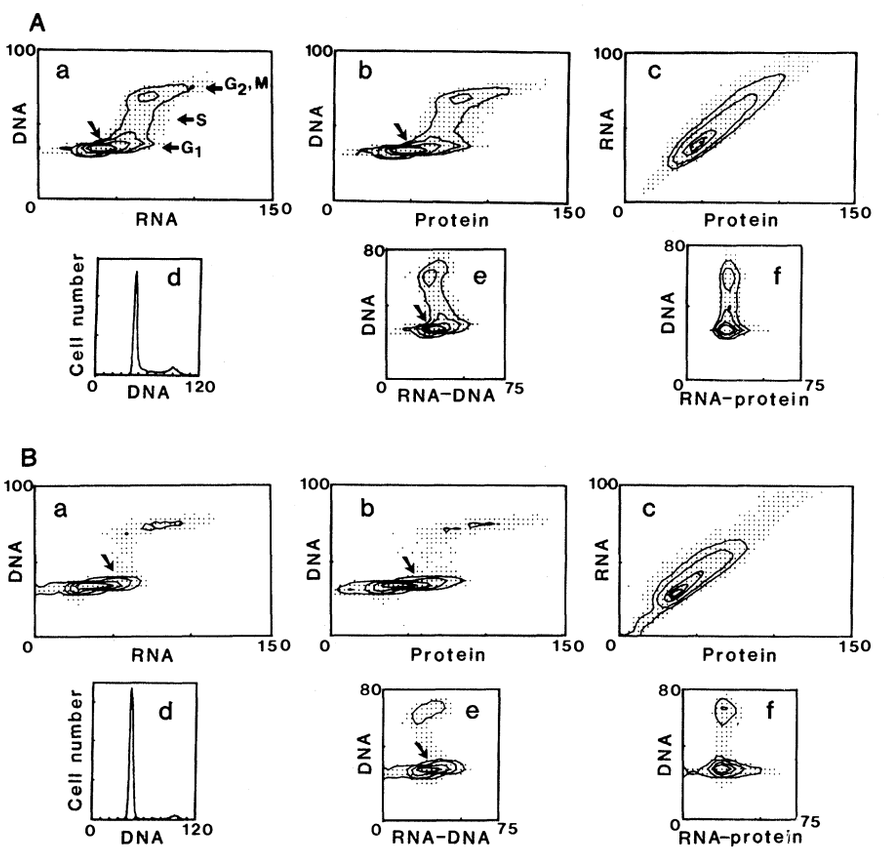

Fig. 2. (A and B) Contour isometric maps (a, b, c, e, and f) and DNA frequency histograms (d) representing the distribution of cells with respect to DNA, RNA, and protein content of CHO cells from exponentially growing cultures (A) and from cultures deprived of isoleucine for 30 hours (B). The shaded areas and the sequential contours represent increasing isometric levels equivalent to 5, 10, 50, 250, 500, and 1500 cells, respectively; 4×10^4 cells were measured per sample. In the exponentially growing population 57, 24, and 19 percent of the cells were in G_1, S, and G_2 + M, respectively, compared to 95, 2, and 6 percent in the isoleucine-deprived population. The arrows indicate the threshold RNA or protein content of G_1 cells; cells with RNA or protein below the threshold values did not immediately enter the S phase.

estimate this ratio, but also to relate it to cell cycle position. The RNA-protein ratio thus provides a useful parameter that can detect unbalanced growth when the rates of RNA and protein accumulation (reflecting DNA transcription and RNA turnover as well as protein synthesis and degradation) vary with respect to each other. No such variability was detected during progression through the cell cycle; as a matter of fact, the RNA-protein ratio remained strikingly constant for all cells regardless of their DNA content (panel f in Fig. 2A). This pattern is expected because a very good correlation between RNA and protein content was seen in individual cells (panel c in Fig. 2A).

Noncycling cells arrested in G_1 by isoleucine deprivation (*13*) showed a much higher heterogeneity in RNA content (panel a in Fig. 2B) and protein content (panel b in Fig. 2B) than cycling, exponentially growing cells. A threshold RNA or protein content similar to that observed in the cycling population was also evident for the G_1 population in the isoleucine-deprived cells (arrows in panels a and b of Fig. 2B). Over 90 percent of these cells had the subthreshold RNA content and may be characterized as G_1A cells (*5*). The mean RNA content of the G_1 population, however, was only slightly lower than that of cycling cells (Table 1). Unlike S cells from the exponentially growing cultures, the very few cells still in the S phase in isoleucine-free cultures did not show an increased RNA content during progression through that phase, as shown by the vertical slope of the S cluster. A good correlation was also observed between RNA and protein content of individual cells (panel c in Fig. 2B), although the distribution was more asymmetric than in exponentially growing cultures.

Similarly, both the RNA-DNA (panel e in Fig. 2B) and RNA-protein (panel f in Fig. 2B) ratio distributions of noncycling isoleucine-deprived cells showed higher heterogeneity in the G_1 population than in the exponentially growing population. Cell distribution with respect to the RNA-protein ratio was less symmetrical than in cycling populations; the skew of the distribution indicates the presence of G_1 cells with lowered protein content but still relatively high RNA. The mean values of RNA and protein, however, were proportionally lower in the cells deprived of isoleucine, as reflected by the nearly identical RNA-protein ratios for these cultures and for cells growing exponentially (Table 1). Thus, by the criterion of RNA-protein ratio, the noncycling cells exhibited, in general, a state of balanced growth despite the fact that their RNA-DNA ratio or protein content was somewhat diminished. It should be emphasized here that the RNA-protein ratio is a sensitive measure of unbalanced growth and, for instance, short treatment of cells with drugs inhibiting either RNA, protein, or DNA synthesis produces a marked change in this ratio (*16*). This novel parameter (RNA-protein ratio versus DNA distribution) may be of particular interest in analysis of growth perturbation induced by drugs.

Table 1. RNA and protein content and RNA-DNA and RNA-protein ratios for G_1, mid-S, and G_2 + M populations of CHO cells from exponentially growing and isoleucine-deprived cultures. The samples were stained (*6*) and measured as described in the text and in the legend to Fig. 1. Populations of G_1, mid-S, and G_2 + M cells were selected on the basis of differences in DNA content by computer iterative programs. The results are expressed in arbitrary units of mean fluorescence intensity (standard deviation) or as ratios of intensities (channel number).

Cell cycle phase	RNA content	Protein content	RNA-DNA	RNA-protein
		Exponentially growing cells		
G_1	57.3 (12.9)	67.4 (16.2)	44.0 (8.8)	35.6 (4.9)
Mid-S	82.7 (12.5)	94.7 (16.0)	46.2 (6.9)	36.9 (4.9)
G_2 + M	100.7 (17.1)	115.1 (21.8)	39.3 (6.3)	36.8 (4.9)
		Noncycling (isoleucine-deprived) cells		
G_1	51.3 (13.5)	59.1 (16.6)	40.3 (9.4)	35.4 (6.7)
Mid-S	72.3 (15.0)	83.6 (20.9)	40.6 (9.3)	36.4 (8.7)
G_2 + M	103.8 (26.0)	119.2 (30.9)	38.9 (8.3)	37.1 (6.3)

One of the advantages of the multivariate correlated data (as shown in Fig. 2) is the possibility of identification of particular cell subpopulations by gating analysis. For instance, we attempted to learn whether the G_1 subthreshold (G_1A) subpopulation discriminated by RNA content is identical with the subthreshold G_1 subpopulation recognized by protein content (panels a and b in Fig. 2A). By gating the subthreshold cells during analysis of DNA and RNA distributions, subsequent reprocessing of the data, and replotting the gated subpopulation in accordance with the DNA and protein distributions, we were able to confirm the identity of these subpopulations. Although this was expected on the basis of the close relation between RNA and protein content (panel c in Fig. 2A), the multivariate gating analysis proved the identity of these subpopulations.

This method has several advantages over currently available techniques. Biochemical estimates of the correlations among DNA, RNA, and protein cannot provide information on individual cells and population heterogeneity; also, it is impossible to correlate RNA-protein ratios with position in the cell cycle. Autoradiography is cumbersome, does not allow the study of large cell populations, and makes it difficult if not impossible to correlate RNA-protein ratios with position in the cell cycle. Use of FITC-labeled antibodies against particular cellular proteins in place of FITC as a general protein stain can allow the content of these specific proteins to be estimated in relation to RNA and DNA.

Changes in RNA content during quiescence may be related to the "depth" of quiescence (*17*) and the type of cell examined (*4*). The metabolic state of noncycling cells obtained from isoleucine-deprived CHO cultures is different from that of quiescent lymphocytes or 3T3 fibroblasts, which remain in a quiescent state with a markedly depressed RNA and protein content (*4*). Thus by criteria proposed before (*4*), noncycling CHO cells from isoleucine-deprived cultures should be considered as being arrested in G_1A rather than as being in deep quiescence (G_1Q). In using this technique to investigate tumor cell growth, differentiation, and drug sensitivity, we have observed that the method offers a powerful approach for analyzing cell heterogeneity and for discriminating among the distinct metabolic states characterized by changeable rates of DNA transcription and translation.

HARRY A. CRISSMAN
Los Alamos National Laboratory, Los Alamos, New Mexico 87545
ZBIGNIEW DARZYNKIEWICZ
Sloan-Kettering Institute for Cancer Research, Rye, New York 10580
ROBERT A. TOBEY
JOHN A. STEINKAMP
Los Alamos National Laboratory

References and Notes

1. M. A. Van Dilla *et al.*, *Science* **163**, 1213 (1969); H. A. Crissman and R. A. Tobey, *ibid.* **184**, 1297 (1974); A. Krishan, *J. Cell Biol.* **66**, 188 (1975).
2. Z. Darzynkiewicz, F. Traganos, T. Sharpless, M. R. Melamed, *Exp. Cell Res.* **95**, 143 (1975); *Proc. Natl. Acad. Sci. U.S.A.* **76**, 358 (1976); K. D. Bauer and L. A. Dethlefsen, *J. Histochem. Cytochem.* **28**, 493 (1980).
3. H. A. Crissman and J. A. Steinkamp, *J. Cell Biol.* **59**, 766 (1973); W. Gohde, I. Spies, J. Schumann, T. Buchner, G. Klein-Dopke, in *Pulse-Cytophotometry*, T. Buchner, W. Gohde, J. Schumann, Eds. (European Press, Ghent, Belgium, 1976), p. 27; H. A. Crissman and J. A. Steinkamp, *Cytometry* **3**, 84 (1982).
4. Z. Darzynkiewicz, F. Traganos, M. R. Melamed, *Cytometry* **1**, 98 (1980); Z. Darzyn-

kiewicz and F. Traganos, in *Genetic Expression in the Cell Cycle*, G. M. Padilla and K. S. McCarty, Sr., Eds. (Academic Press, New York, 1982), p. 103.
5. Z. Darzynkiewicz, T. Sharpless, L. Staiano-Coico, M. R. Melamed, *Proc. Natl. Acad. Sci. U.S.A.* **77**, 6696 (1980); Z. Darzynkiewicz, H. A. Crissman, F. Traganos, J. Steinkamp, *J. Cell Physiol.* **113**, 465 (1982).
6. Effects of dye concentrations, staining time, temperature, and *p*H were determined for three-color staining and analysis of DNA, RNA, and protein in ethanol-fixed CHO cells with the dyes Hoechst 33342, pyronin Y (PY), and fluorescein isothiocyanate (FITC), respectively. Results were used to assess optimum conditions for cell staining. Cycling and noncycling populations of CHO cells were harvested from suspension cultures by centrifugation. The culture medium was aspirated and the cells were fixed in 70 percent cold ethanol for at least 12 hours and then centrifuged. The ethanol was removed and the cells were resuspended in phosphate-buffered saline (PBS; *p*H 7.4) containing Hoechst 33342 (0.5 μg/ml) and FITC (0.1 μg/ml) and stained for at least 30 minutes at room temperature. The staining tubes were then chilled on ice for at least 5 minutes and an equal volume of cold PBS staining solution containing Hoechst 33342 (0.5 μg/ml), FITC (0.1 μg/ml), PY (2.0 μg/ml) was added to the suspension of stained cells. After 5 minutes of staining on ice cells were analyzed in the dye solution in an ice bath. Final cell concentration was maintained at approximately 7.5×10^5 cells per milliliter for analysis in the three-laser system (*9*).
7. D. Arndt-Jovin and T. M. Jovin, *J. Histochem. Cytochem.* **25**, 589 (1977).
8. J. Brachet, *C. R. Soc. Biol.* **133**, 88 (1940); H. J. Tanke, I. A. B. Nieuwenhuis, G. J. M. Koper, J. C. M. Slats, J. S. Ploem, *Cytometry* **1**, 313 (1981); H. M. Shapiro, *ibid.* **2**, 143 (1981); A. Pollack *et al.*, *ibid.* **3**, 38 (1982).
9. J. A. Steinkamp, C. C. Stewart, H. A. Crissman, *Cytometry* **2**, 226 (1982).
10. J. A. Steinkamp and R. D. Hiebert, *ibid.* **2**, 232 (1982).
11. G. C. Salzman, S. F. Wilkins, J. A. Whitfill, *ibid.* **1**, 325 (1981).
12. Chinese hamster cells (line CHO, originally obtained from T. T. Puck) were maintained in exponential growth phase in suspension culture free of mycoplasma contamination in Ham's F-10 medium supplemented with heat-inactivated newborn calf serum (15 percent), penicillin (100 U/ml), and streptomycin (100 μg/ml). CHO cells were synchronized in the G_1 phase by continuous growth for 30 hours in isoleucine-free F-10 medium containing thrice-dialyzed newborn calf serum (15 percent).
13. R. A. Tobey, *Methods Cell Biol.* **6**, 67 (1973).
14. T. Lindmo, *Cell Tissue Kinet.* **15**, 197 (1982).
15. R. Baserga, *Exp. Cell Res.* **151**, 1 (1984).
16. H. A. Crissman, Z. Darzynkiewicz, R. A. Tobey, J. A. Steinkamp, *J. Cell Biol.*, in press.
17. R. Baserga, *J. Cell Physiol.* **95**, 3777 (1978); L. H. Augenlicht and R. Baserga, *ibid.* **89**, 255 (1974).
18. This work was performed under the auspices of the Los Alamos National Flow Cytometry and Sorting Research Resource funded by the Division of Research Resources of NIH (grant P41-RR01315-02), the Department of Energy, and PHS grants 1R0CA23296 and CA 28704.

13 November 1984; 19 December 1984

Angiogenesis Induced by Degradation Products of Hyaluronic Acid

Abstract. *Partial degradation products of sodium hyaluronate produced by the action of testicular hyaluronidase induced an angiogenic response (formation of new blood vessels) on the chick chlorioallantoic membrane. Neither macromolecular hyaluronate nor exhaustively digested material had any angiogenic potential. Fractionation of the digestion products established that the activity was restricted to hyaluronate fragments between 4 and 25 disaccharides in length.*

Hyaluronic acid has been implicated in cell-cell interaction, cell-matrix adhesion, cell motility, and the ordering of the extracellular matrix (*1, 2*). In many developing or remodeling tissues a hyaluronate-rich stroma accompanies cell migration (*1*). Subsequent differentiation and vascular ingrowth are associated with an increase in tissue hyaluronidase activity and a decrease in hyaluronic acid concentration (*3*). Hyaluronate inhibits vascularization of chick embryo limb buds (*4*) and delays or reduces development of granulation tissue and newly formed capillaries around subcutaneous implants (*5*). In this report we describe a further regulatory role for certain products of hyaluronate degradation.

Preparations of both human umbilical (Miles Scientific 36-242-1; Sigma H1751) and bovine vitreous (Sigma H7630) hyaluronic acid were used to minimize the possibility of artifacts produced by contaminating species. Because the major contaminants in such preparations are normally chondroitin 4- and 6-sulfate, a mixed preparation of these (Sigma C3219) was also tested. Each glycosaminoglycan preparation was subjected to enzymatic digestion. Testicular hyaluronidase (Miles Scientific 32-042-1) digests were carried out in 0.1*M* acetate buffer and 0.15*M* NaCl (*p*H 5.4) at an enzyme-to-substrate ratio of 1 to 2 by weight (125 to 250 turbidity-reducing units per milligram of substrate). These were incubated at 37°C for the periods indicated in Table 1, and the reaction was stopped by inactivating the enzyme at 100°C for 5 minutes. The digests were then centrifuged at 2000*g* for 10 minutes, filtered through a glass fiber filter (pore size, 1 μm), and freeze-dried.

We determined angiogenic activity by the chick chorioallantoic membrane (CAM) assay (Fig. 1) (*6*). Hyaluronic acid preparations digested with testicular hyaluronidase for 1 to 10 hours consistently gave a significantly higher proportion of positive responses than undigested control preparations ($P < 0.0003$, χ^2 test). However, 24-hour digests showed largely negative responses and did not differ significantly from the controls. CAM assays with hyaluronic acid and heat-denatured hyaluronidase were also negative. Commercial preparations of hyaluronidase have been reported to be contaminated with a vascular permeability factor (*7*). However, the negative results with denatured hyaluronidase, undigested hyaluronic acid, and the 24-hour digest eliminate this as a major factor in the angiogenic response observed. The possibility that chondroitin sulfate contaminants caused the angiogenic activity is not supported by the results (Table 1).

To further test the hypothesis that the angiogenic activity was due to hyaluronate fragments, we incubated 16 mg of the angiogenic hyaluronate digest for 16 hours with 1000 U of streptomyces hyaluronidase (Sigma H1136) at *p*H 5.0 and 60°C. The reaction was stopped by adding cold trichloroacetic acid, the digest was centrifuged (2000*g* for 30 minutes at 4°C), and the supernatant was exhaustively dialyzed against distilled water and freeze-dried. Hyaluronate digest was also carried through the same procedure without the hyaluronidase. The latter preparation was still angiogenic in the CAM assay, but the streptomyces hyaluronidase digest was not. Since streptomyces hyaluronidase is specific for hyaluronic acid, this is further evidence that the angiogenic component of the original digests is derived from hyaluronate.

An exhaustive digest (24 hours) of hyaluronate with testicular or streptomyces hyaluronidase yields essentially a mixture of tetra- and hexasaccharides.

Table 1. Angiogenic activity of hyaluronidase digests. Numbers in parentheses give the number of preparations tested.

Material tested	Number of eggs showing positive angiogenesis/total number of eggs*			
	No digestion	1 to 2 hours	4 to 10 hours	>24 hours
Hyaluronic acid	3/23 (9)	28/45 (18)	41/45 (18)	4/19 (7)
Chondroitin 4- and 6-sulfate	1/8 (5)	3/24 (10)	2/16 (7)	0/10 (5)

*Control results: heat-inactivated hyaluronidase, 4/18 (7); hyaluronidase buffer, 1/13 (6); native hyaluronate, 3/25 (10); native chondroitin 4- and 6-sulfate, 4/19 (7).